8-19-1966

# Surface-Wave Phenomena At A Water-Air Interface.

Benjamin W. Woodward

# SURFACE - WAVE PHENOMENA AT A WATER - AIR INTERFACE

By

Benjamin W. Woodward

A Thesis

Submitted in Partial Fulfillment of the

Requirements for the Degree of

Master of Science in Physics

The University of New Mexico

1966

This thesis, directed and approved by the candidate's committee, has been accepted by the Graduate Committee of the University of New Mexico in partial fulfillment of the requirements for the degree of

MASTER
OF
SCIENCE IN PHYSICS

Sidney Rosenblum
Dean

Date August 19, 1964

SURFACE-WAVE PHENOMENA AT A WATER-AIR INTERFACE

by

BENJAMIN W. WOODWARD

Thesis committee

Howard C. Bryant
Chairman

Robert H. Koch

Christopher Dean

ACKNOWLEDGEMENTS

The author wishes to thank the Air Force Weapons Laboratory for the loan of their helium-neon laser, T. R. Bonner for the loan of his camera, and T. Fahlen for his helpful suggestions. The author is especially grateful to Dr. H. C. Bryant for his interest in this project, for his advice, and for many beneficial discussions of these experiments.

TABLE OF CONTENTS

## LIST OF ILLUSTRATIONS

## INTRODUCTION

The existence of a surface wave accompanying total internal reflection of light in a dielectric material was derived classically to satisfy boundary conditions at the surface[1]. Using this fact, in 1929 J. Picht [2] proposed a mechanism for total reflection that led to the conclusion that a finite ray of light would undergo a small translation at the boundary, parallel to the boundary and in the plane of incidence. In 1943 Goos and Hänchen [3] made quantitative measurements of this translation or shift. Subsequently many theories have been advanced analyzing this phenomenon in detail[4,5], but as of this writing no other experimental evidence has been reported.

In addition to a shift of the center of a beam of the order of a micron in the reflection of a ray of light, other experiments with light incident at angles very near the critical angle have indicated the presence of "surface waves" carrying significant quantities of energy over distances as far as several centimeters before re-entering the denser medium[6]. It is not known whether such waves are of the same type as those accompanying total reflection; however, they may play a role in a type of scattering from water droplets as observed in the glory phenomenon[7].

The purpose of this project is to investigate surface wave phenomena at a plane horizontal water-air interface in support of other experiments on the back scattering of light from water droplets

[7]. In this context, the main objectives are to detect and measure surface waves and/or their effects, such as the Goos-Hänchen shift. A helium-neon gas laser is called for to provide light of the same wavelength as used in the other experiments and to obtain the best combination of desirable characteristics of the light ray.

## THEORETICAL CONSIDERATIONS

Although the theory of reflection and refraction are treated in standard texts, the following diagrams and equations are included for the purpose of definition:

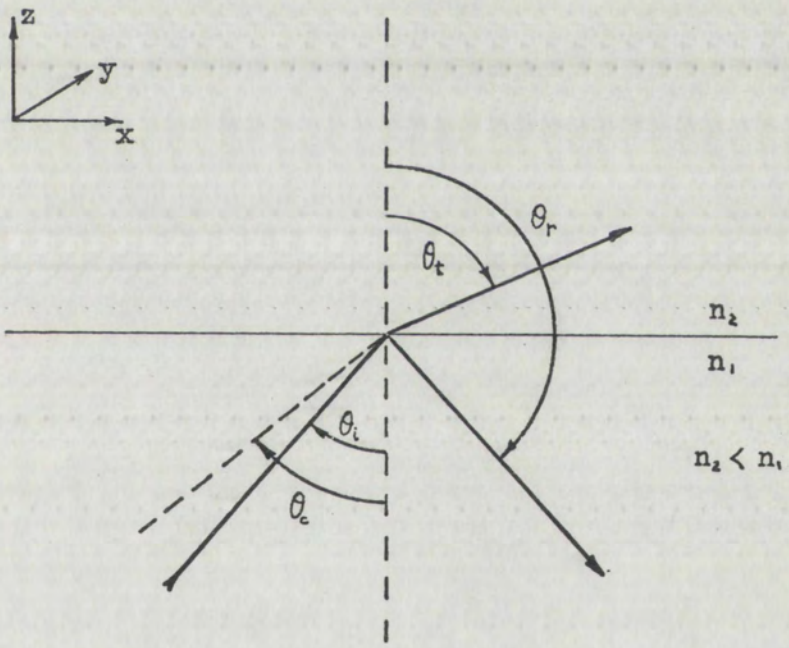


Figure 1. Reflection and Refraction

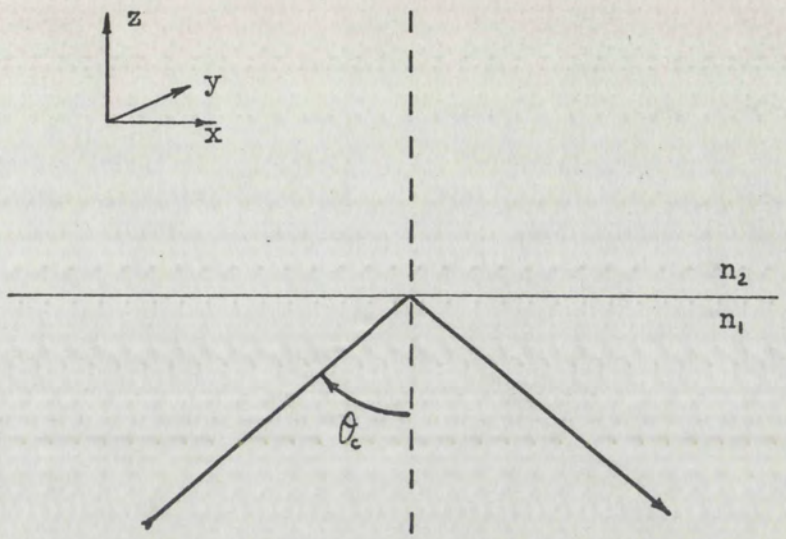


Figure 2. Reflection at the Critical Angle

From Snell's Law one obtains

$$n_1 \sin \theta_i = n_2 \sin \theta_t ; \qquad (1)$$

and, in the case of reflection at the critical angle,

$$\sin \theta_c = \frac{n_2}{n_1} . \qquad (2)$$

Since the quantity appears frequently, it is convenient to define $n = n_2/n_1$.

Surface Waves

The imposition of boundary conditions on a light wave at the boundary between two non-absorbing dielectric media leads to a surface or evanescent wave in the case of total internal reflection. The boundary conditions are that the tangential components of the electric and magnetic vectors be continuous across the boundary between the media. Thus, even if the light is incident at an angle greater than

or equal to the critical angle and is totally reflected, electric and magnetic fields must exist in the rarer medium. According to Born and Wolf [1], this field

$$S \propto \exp\left[-i\omega\left(t - \frac{x \sin\theta_i}{n v_2}\right)\right] \cdot \exp\left[\mp \frac{\omega z}{v_2}\sqrt{\frac{\sin^2\theta_i}{n^2} - 1}\right] \qquad (3)$$

represents a non-homogeneous wave propagated along the boundary in the plane of incidence (x-direction). In the event that the second medium can be considered to extend to infinity, only the minus sign in front of $\omega z$ is allowed. This wave is not transverse, for the field is non-zero in the direction of propagation. This formula is the steady state solution and assumes an infinite plane wave incident on the boundary. J. Picht obtains a similar result for a finite beam by assuming cylindrical waves and then showing that the center of any such beam can be approximated by plane waves [5].

F. I. Fedorov [4] considers a more general case of polarization of the incident light and shows that for arbitrarily polarized light, the surface wave in the rarer medium is no longer directed parallel to the plane of incidence but has a component perpendicular to the plane of incidence. Fedorov asserts that, although the Poynting vector $\vec{P}$ can be separated into components parallel and perpendicular to the plane of incidence, in general these components of the reflected and refracted waves are not proportional to the corresponding components of the incident wave, because $\vec{P}$ depends quadratically on the vectors $\vec{E}$ and $\vec{H}$. He points out that the differences between results such as Born and Wolf's (which are valid for the incident light polarized

parallel or perpendicular to the plane of incidence) and the results obtained by considering a more general case of polarization are due to that fact. Accordingly, Fedorov develops the entire theory of reflection and refraction in vector form (refer to Appendix I for a review of Fedorov's treatment). He obtains an expression for the Poynting vector in the rarer medium,

$$\vec{P}_2 = \frac{c}{16\pi}\left\{\left[\vec{E}_2^{\,2}\,\vec{m}_2 + \vec{E}_2^{\,*2}\,\vec{m}_2^{\,*}\right] + \left[|\vec{E}_2|^2(\vec{m}_2 + \vec{m}_2^{\,*}) - (\vec{m}_2 - \vec{m}_2^{\,*}) \times (\vec{E}_2 \times \vec{E}_2^{\,*})\right]\right\}, \qquad (4)$$

where $\vec{E}_2$ is the electric vector in the rarer medium, and $\vec{m}_2$ is the index of refraction $n_2$ times the unit vector normal to the wave front. As shown in Appendix I, $\vec{E}_2$ and $\vec{m}_2$ are derivable from the parameters of the incident ray through the laws of reflection and refraction and the Fresnel formulae. The component of $\vec{P}_2$ perpendicular to the plane of incidence is contained in the term $(\vec{m}_2 - \vec{m}_2^{\,*}) \times (\vec{E}_2 \times \vec{E}_2^{\,*})$. This term vanishes if $\vec{m}_2 = \vec{m}_2^{\,*}$ ($\vec{m}_2$ is complex only in the case of total reflection) or if $(\vec{E}_2 \times \vec{E}_2^{\,*}) = 0$. This latter situation is a condition for linearly polarized light, which is produced if the incident ray is linearly polarized parallel or perpendicular to the plane of incidence. The quantity $(\vec{E}_2 \times \vec{E}_2^{\,*})$ also equals zero for a particular phase difference of elliptical polarization of the incident ray.[1]

The surface waves considered above transport energy along the surface of the denser medium, but only in the region where an ordinary

---

[1] Fedorov's results have not been incorporated in the latest edition of Born and Wolf [1] or in Rossi's Optics [8], although they have been used in further theoretical work by H. Schilling [9].

transverse wave is reflected on the other side of the interface. Such surface waves exist to satisfy boundary conditions and in turn cannot exist together with a single plane refracted wave due to similar boundary conditions. Nevertheless, experiments by Osterberg and Smith [6] indicate a flow of energy parallel to the surface. Because of the boundary condition problem and because some of their experiments indicate that this transport of energy does not occur by surface waves of the above type, Osterberg and Smith suggest that these apparent surface waves are in fact transverse waves arising from diffraction effects of the incident beam at the boundary between the media. This transport of energy is sharply peaked at an angle of incidence one second less than the critical angle. These waves are detected by observing light re-entering the first medium at the critical angle. Such a phenomenon should not occur for transverse waves just grazing a surface, although microscopic surface imperfections could cause irregular behavior. It seems evident that there is much room for further investigation of surface wave phenomena.

Polarization

The information regarding polarization of reflected and refracted waves is contained in the Fresnel equations or in the development by Fedorov. Results pertinent to these experiments are stated here. If linearly polarized light is incident on the surface at less than the critical angle, the refracted and reflected rays are both linearly polarized but not at the same angle, $\chi$, to the plane of incidence as the incident wave, unless the incident ray is polarized parallel or perpendicular to the plane of incidence; i.e., $\chi = 0$ or $\pi/2$. In the latter case, the reflected and refracted waves remain polarized in the

same direction at all angles of incidence. If, however, linearly polarized light is incident at an angle greater than critical with $\chi$ between 0 and $\pi/2$, the reflected wave is elliptically polarized. The relative phase differences, $\delta$, is given by the transcendental equation

$$\tan \frac{\delta}{2} = \frac{\cos \theta_i \sqrt{\sin^2 \theta_i - n^2}}{\sin^2 \theta_i} , \qquad (5)$$

where $n = n_2/n_1$ as before [1]. This formula gives an imaginary phase difference if $\theta_i < \theta_c$, $\delta = 0$ if $\theta_i = \theta_c$ or if $\theta_i = \pi/2$, and positive values of $\delta$ for all intermediate values of $\theta_i$. It will be of interest to develop an expression relating $\delta$ and a difference of only a few minutes of arc between the critical angle and the angle of incidence. Since $\tan \delta/2 \to 0$ as $\theta_i \to \theta_c$, assume that the approximation

$$\tan \frac{\delta}{2} = \frac{\delta}{2} \qquad (6)$$

will be valid. Let $\theta_i = \theta_c + \varepsilon$ where $\varepsilon \ll \theta_c$. One obtains

$$\frac{\delta}{2} = \frac{\cos(\theta_c + \varepsilon) \sqrt{\sin^2(\theta_c + \varepsilon) - n^2}}{\sin^2(\theta_c + \varepsilon)} . \qquad (7)$$

Expanding the trignometric functions,

$$\cos(\theta_c + \varepsilon) = \cos\theta_c \cos\varepsilon - \sin\theta_c \sin\varepsilon ; \qquad (8)$$

$$\sin(\theta_c + \varepsilon) = \sin\theta_c \cos\varepsilon + \sin\varepsilon \cos\theta_c ; \qquad (9)$$

$$\sin^2(\theta_c + \varepsilon) = \sin^2\theta_c \cos^2\varepsilon + 2 \cos\theta_c \sin\theta_c \cos\varepsilon \sin\varepsilon + \cos^2\theta_c \sin^2\varepsilon . \qquad (10)$$

Recall that $\sin\theta_c = n$. It will be sufficient to consider only first order terms in $\varepsilon$. The following equation is obtained:

$$\frac{\delta}{2} = \frac{(\cos\theta_c - n\varepsilon)\sqrt{2n\varepsilon\cos\theta_c}}{n^2 + 2n\varepsilon\cos\theta_c} \quad ; \tag{11}$$

$$\therefore \frac{\delta}{2} = \frac{\sqrt{(\cos^2\theta_c - 2n\varepsilon\cos\theta_c + n^2\varepsilon^2)(2n\varepsilon\cos\theta_c)}}{n^2 + 2n\varepsilon\cos\theta_c} \quad . \tag{12}$$

Still neglecting terms of higher order in $\varepsilon$ than first,

$$\frac{\delta}{2} = \frac{\sqrt{2n\varepsilon\cos^3\theta_c}}{n^2 + 2n\varepsilon\cos\theta_c} \quad . \tag{13}$$

Squaring both sides and re-arranging

$$\left(n^2 + 2n\varepsilon\cos\theta_c\right)^2 \frac{\delta^2}{4} = 2n\varepsilon\cos^3\theta_c \quad ; \tag{14}$$

$$\therefore \quad n^4\delta^2 + 4n^3\varepsilon\cos\theta_c\,\delta^2 = 8n\varepsilon\cos^3\theta_c \quad ; \tag{15}$$

$$\therefore \quad \varepsilon\left(8n\cos^3\theta_c - 4n^3\cos\theta_c\,\delta^2\right) = n^4\delta^2 \quad ; \tag{16}$$

$$\therefore \quad \varepsilon = \frac{n^3\delta^2}{4\cos\theta_c\,(2\cos^2\theta_c - n^2\delta^2)} \quad . \tag{17}$$

Moreover, since $n^2\delta^2 \ll 2\cos^2\theta_c$, neglect $n^2\delta^2$ in the denominator of (17), so that

$$\varepsilon = \left(\frac{n}{2\cos\theta_c}\right)^3\delta^2 \quad ; \tag{18}$$

or,

$$\varepsilon = \frac{1}{8}\tan^3\theta_c\,\delta^2 \quad . \tag{19}$$

The term $\tan^3 \theta_c$ and other terms in the expressions above are of the order of unity for light reflected from a water-air interface; therefore, the approximations used in the derivation are valid for angles $\varepsilon \ll 1/8$.

## APPARATUS

The experiments generally are conducted in the following configuration: The laser beam is directed at a water surface at an angle such that the incident beam is near the critical angle. Observations are made of the refracted and reflected beams both visually and with a photoconductive cell. A lens is used to direct light emerging parallel to and above the reflected beam to a very sensitive photoconductive cell.

### Laser

The light source is a Perkin-Elmer 5200 helium-neon gas laser. The characteristic wavelength of this type laser is 6328 Å. The power rating is ~.5 mw, and the angular divergence is measured to be 4.1 ± 0.3 minutes. This value is somewhat larger than that hoped for; furthermore, the beam shape is elliptical, becoming noticeable at distances greater than approximately 2 m. The ratio of the major and minor axes of the ellipse, as determined from photographs taken of the beam cross-section, is 3:2. The angular divergence is given for the spread along the major axis.

A much more serious deficiency is that the laser beam is surrounded by other light of the same wavelength and of appreciable magnitude. This extra light has a well-defined but irregular pattern suggestive of diffraction interference. It has a measurable effect on almost all experiments attempted and a strong effect on the most successful

experiment. This light emerges form the laser coincident with the main beam so that attempts to block the unwanted light near the source result in partial covering of the main beam with the accompanying diffraction patterns, without completely eliminating the off-axis noise. Good results in eliminating this extraneous light are obtained with one pinhole 2.52 mm in diameter at 83 cm from the laser. Supporting the aluminum plate with this pinhole is a heavy black paper tube connected to the laser. The tube can be adjusted to center the pinhole exactly on the beam. This arrangement has the advantage of moving the hole with changes in angle of the laser beam, a desirable feature in all measurements, but mandatory in observing surface wave phenomena.

The laser itself is mounted on a steel milling head, which is mounted to move in a vertical plane. A small handwheel turns the main wheel nine degrees per revolution with a worm and pinion gear mechanism. Scale markings on the handwheel are at 3 minute intervals. Although no vernier is incorporated, interpolation could in principle give rather precise angle measurements. An accurate zero could be attained by aligning the laser beam with the water surfaces in two jars separated by 5 m and connected by a siphon tube. It is estimated that the maximum uncertainty in establishing the zero angle by this method would be less than 8 seconds. Unfortunately, the backlash in the wheel gear drive is at least 3 minutes; consequently, precise angle measurements can not be made. Relative angles can be measured with good precision providing the laser wheel is rotated in only one direction for a series of measurements.

Water Surface

It is desired to use the cleanest, stillest possible water sur-

face to reflect the laser light. An ordinary five gallon aquarium tank is filled with distilled water to a depth of approximately 14 cm. The top of the tank is covered with two layers of polyethylene plastic. The entire tank is mounted on a jack with which one can move the tank up and down. The jack in turn is screwed to a wood platform which rests on a partially inflated inner tube (see Figure 3.) The function of the inner tube is to provide insulation against building vibration; however, it does not entirely eliminate vibration, and it does make the water surface very unstable against accidental jarring of the tank or the mounting apparatus. It would be worthwhile to investigate supplementary and alternate methods of reducing vibration of the water surface.

Of greater concern to the experiments performed is cleanliness of the water surface, a problem which is complicated by the need to insert other apparatus into the tank besides water: water-resistant black paper at the water level on the entrance and exit sides and on the tank floor and a thermometer. Once the plastic cover is finally in place, however, no further deterioration of the surface occurs. The procedure which gives the cleanest surface is as follows: The tank is carefully washed and dried inside and out and the plastic cover put on. The empty tank and the apparatus to be inserted are carried to a "clean room" where as much as possible of the dust on the apparatus and inside the tank is removed. The apparatus is then put in place inside the tank and the plastic cover replaced. The clean tank is carried back to the laboratory where distilled water is siphoned into the tank without removing the cover. After filling, removal of the cover for any reason generally leads to a dustier

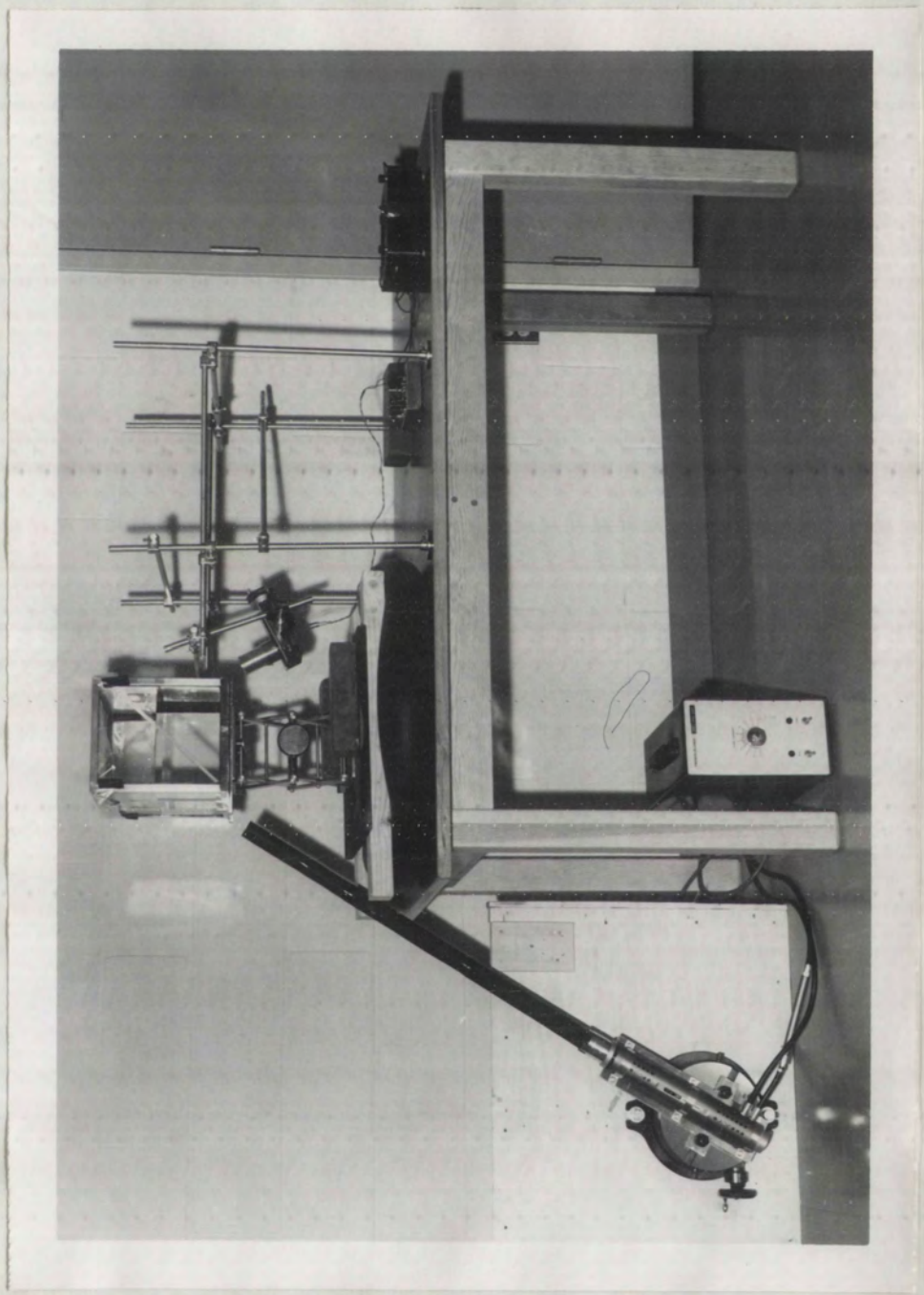

Figure 3. Arrangement of Apparatus

water surface.

Detectors

The detecting equipment consists of a lens-photoconductive cell combination, a nicol prism in conjuction with various light detectors, a microammeter, and a Hasselblad 1000F camera. The human eye is a photo-detector of excellent sensitivity and is used extensively in all phases of the experiments.

The lens-photocell combination is designed to select only parallel rays to be received by a Clairex CL 704L photoconductive cell (see Figure 4.). Since only parallel rays converge at the focal point of a

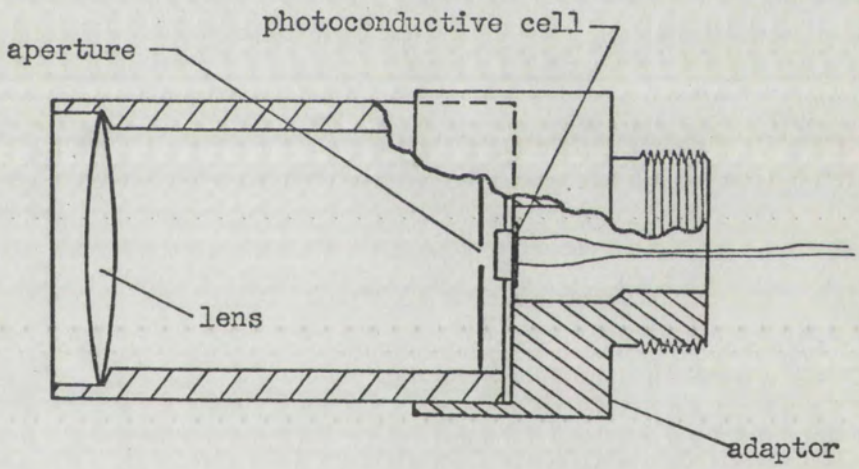


Figure 4. Lens - Photoconductive Cell Combination

simple convex lens, other rays can be prevented from reaching the detector by placing it at the focal point and blocking off any light other than that passing through the lens. An aluminum cylinder is constructed with a recessed portion at one end to receive a 5 cm focal length double convex lens. The effective diameter of the lens in this position is 3.2 cm. A plate is made to fit over the opposite end;

this plate contains a hole which positions the photocell at the focal point. Since the receiving area of the photocell is larger than the image size at that point, an aperture of smaller diameter can be placed at the focal point and the photocell positioned farther from the lens to make use of its full receiving area. An adaptor then fastens this cylinder to an adjustable microscope slide so that the lateral position of the lens and photocell can be measured with precision. The slide incorporates a worm and rack gear mechanism to transform rotation of a graduated wheel to lateral motion of the slide. One revolution of the wheel moves the slide one millimeter, and there are one hundred graduations on the wheel, permitting direct measurement in ten micron intervals.

The CL 704L photoconductive cell is discovered to have different properties, depending not only upon its light history but also on its applied-voltage history. The cell is usually operated beyond the lower limit of the manufacturer's conductance vs illumination curves; in that region there appears to be a large increase in the slope of the conductance vs illumination line after prolonged exposure to light. (This change is of a different type than that stated by the manufacturer.) A more gradual effect is a change in one of the parameters of the photoconductive cell after voltage has been applied over a period of several hours. The conductance G of a photocell is a function of the illumination received and, over relatively small intervals, takes the form $G = L^{\gamma}$ where L is the illumination and $\gamma$ is a number of the order of unity. Evidence is obtained that $\gamma$ is near 1 early after voltage is applied to the cell but increases after several hours in a circuit, whether or not the cell is exposed to light. The characteristics of

the CL 704L cell are measured after voltage has been applied for 4 days. (During this period much more consistent experimental results are obtained than when the cell is turned on and off several times a day.). To determine the value of $\gamma$, it is necessary to measure the conductance of the cell as a function of the intensity of light at the cell. With the laser beam as the source, a nicol prism is used to analyze the beam with the $\vec{E}$ vector of the laser light approximately perpendicular to the principal axis of the nicol prism. The resulting illumination is directly proportional to $\cos^2\phi$, where $\phi$ is the angle between the electric vector of the laser beam and the axis of the nicol prism. Let the photocurrent be designated I; then, when log I is plotted vs log $(\cos^2\phi)$, a straight line of slope $\gamma$ is obtained (see Figure 5.). There is, however, an uncertainty in its behavior at very low illumination levels because the extraneous light from the laser adds a large background current, which does not vanish as $\phi \rightarrow 90°$. When the background current is an order of magnitude larger than the signal current, the data points obtained are not very reliable. The best value for $\gamma$ is $1.20 \pm .044$.

Other photoconductive cells are used in some experiments. A Clairex CL 504L cell can be used in place of the CL 704L cell with a few simple modifications to the lens-photocell apparatus. An RCA 4413 cell is used in experiments with the reflected beam; it has a higher voltage rating and a smaller power rating than the above cells. With a DPDT switch, the same circuit panel can be used for both types of photocells employed. Circuit diagrams for these cells and the microammeter shunts are given in Appendix II.

The nicol prism is employed to analyze the reflected ray and

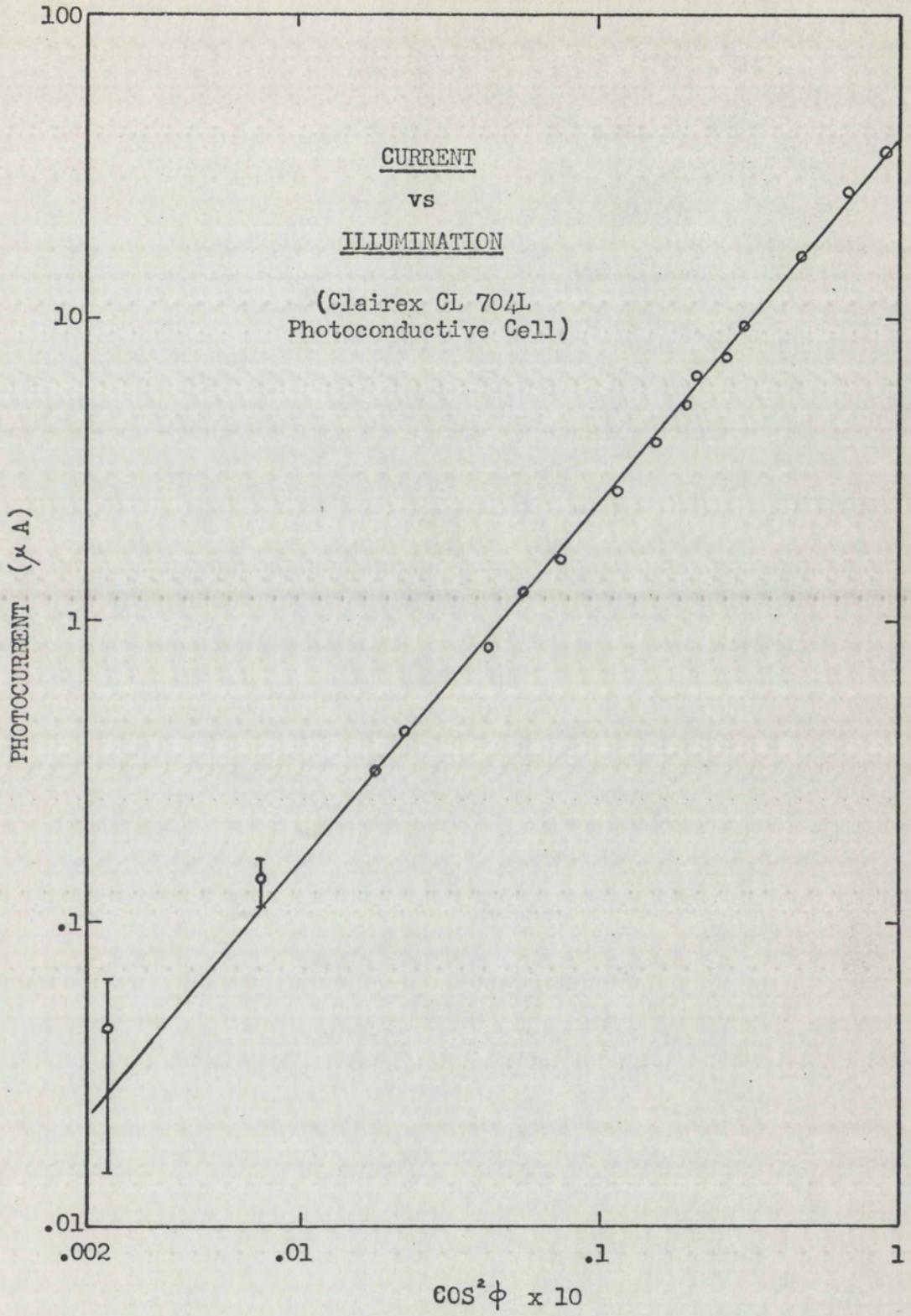


Figure 5. Detector Current vs Illumination

other light to determine polarization characteristics. This device is set either to minimize or to maximize the light intensity. The Hasselblad 1000F camera is used to photograph the cross section of the reflected laser beam. The camera lens is removed and placed a distance in front of the camera to diverge the beam; the camera itself is operated with no lens, which is possible since this model is equipped with a focal plane shutter.

## EXPERIMENTS AND RESULTS

The primary purpose of these experiments is to detect evidence of surface waves at the water-air boundary. As a related topic, measurement of the index of refraction of distilled water would be a desirable by-product. Some experiments are conducted to make a determination of the critical angle, but the results are not conclusive and represent only a minor part of the purpose of the project; consequently, the description of these experiments is contained in Appendix III. Photographs are taken of the reflected beam to try to discover an irregularity in the beam cross section that could be related to the Goos-Hänchen shift. These experiments are also inconclusive and are summarized in Appendix IV. In what is by far the most significant of the experiments, light emerging parallel to the reflected beam is detected when the incident light is very near the critical angle, and its properties are measured. Because of considerations to be discussed, this light is considered to have traveled along the surface before re-entering the water at the critical angle, in the manner discussed by Osterberg and Smith [6]. The effect is observed to be more pronounced when the incident beam is linearly polarized with the electric vector parallel to the plane of incidence than with it perpendicular to the plane of incidence. The illumination produced by the observed light is estimated to be of the order of $10^{-3}$ footcandles, compared with $10^{-4}$ fc for a dark, clear, moonless night, and

about 1 fc for a normally lighted room.

The experimental arrangement is as follows: The lens and photocell apparatus is mounted above the reflected beam in the manner shown in Figure 6. The laser angle is adjusted to bring about reflec-

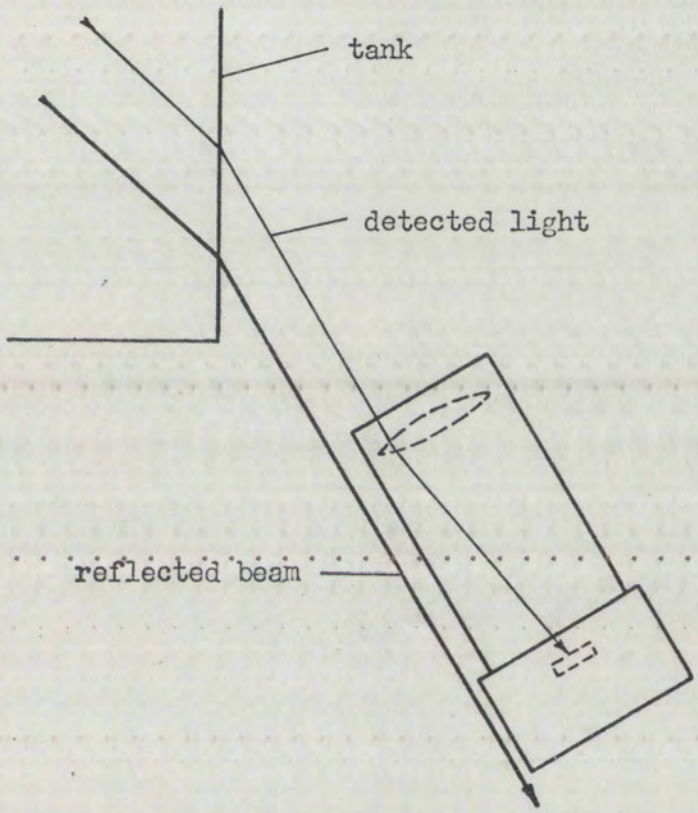


Figure 6. Surface Wave Detection

tion near the critical angle, usually as determined visually. The edge of the lens-photocell holder is aligned parallel to the reflected beam either by observing grazing of the beam along the holder or by use of a direct measuring scale at the top and bottom. Then, with the room darkened, the current in the photoconductive cell is monitored as the angle of the incident beam is varied through the critical angle. At a point intermediate between total reflection and a clear case of partial reflection, a sharp increase in current is

observed, followed by an equally sharp decrease with a further change in the laser angle.

Surface Wave Properties

The most prominent feature of the observed signal is its narrowness with respect to the angle of incidence. As shown in Figures 7, 8, and 9, the entire phenomenon is contained within 3 to 5 minutes of the laser angle, which is in close correspondence with the angular divergence of the laser beam. The signal width varies with the polarization of the incident light because the axis of the elliptical cross section makes different angles with the plane of incidence (since the laser itself is rotated to change the angle of polarization). In several experiments the laser angle is changed over as much as 30 minutes with changes in the background level less than 20 percent, whereas the intensity at the peak near the critical angle is as large as five times the background level.

The intensity of the observed light is a function of the polarization of the incident light. With the incident beam polarized with the electric vector parallel to the plane of incidence, the intensity is greater than it is with the $\vec{E}$ vector perpendicular, the amount depending on the distance from the beam. Further evidence of the dependence on polarization is found by analyzing the light with a nicol prism just before it enters the lens. If the incident light is polarized parallel ($\chi = 0°$) or perpendicular ($\chi = 90°$) to the plane of incidence, the detected light is similarly polarized. But when the incident ray is polarized at an angle $\chi = 45°$ to the plane of incidence, $\chi$ of the detected light is measured to be $\sim 37\frac{1}{2}°$, indicating that the parallel component of the incident light is dominating the effect.

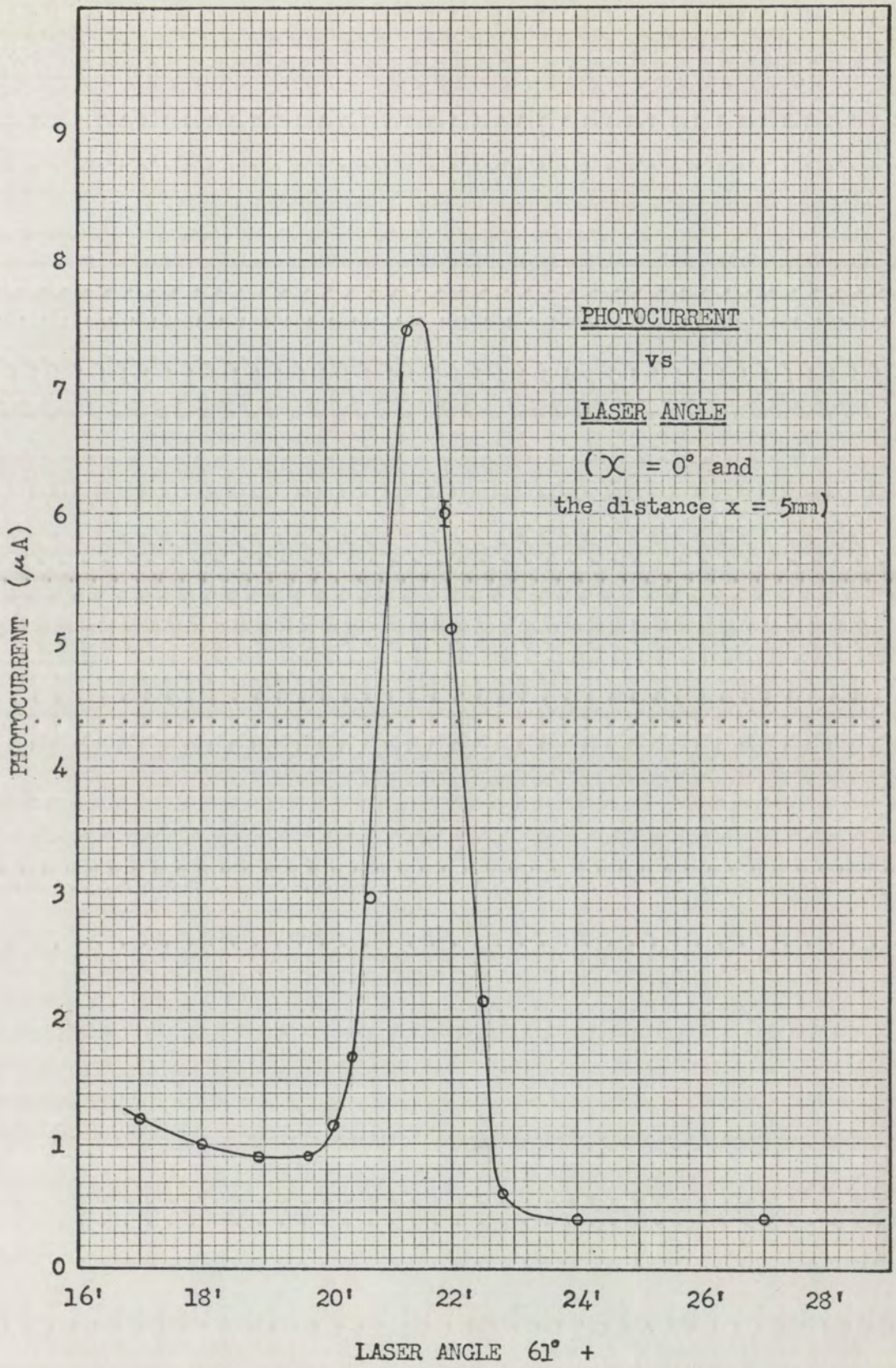


Figure 7. Intensity vs Laser Angle, $\chi = 0°$

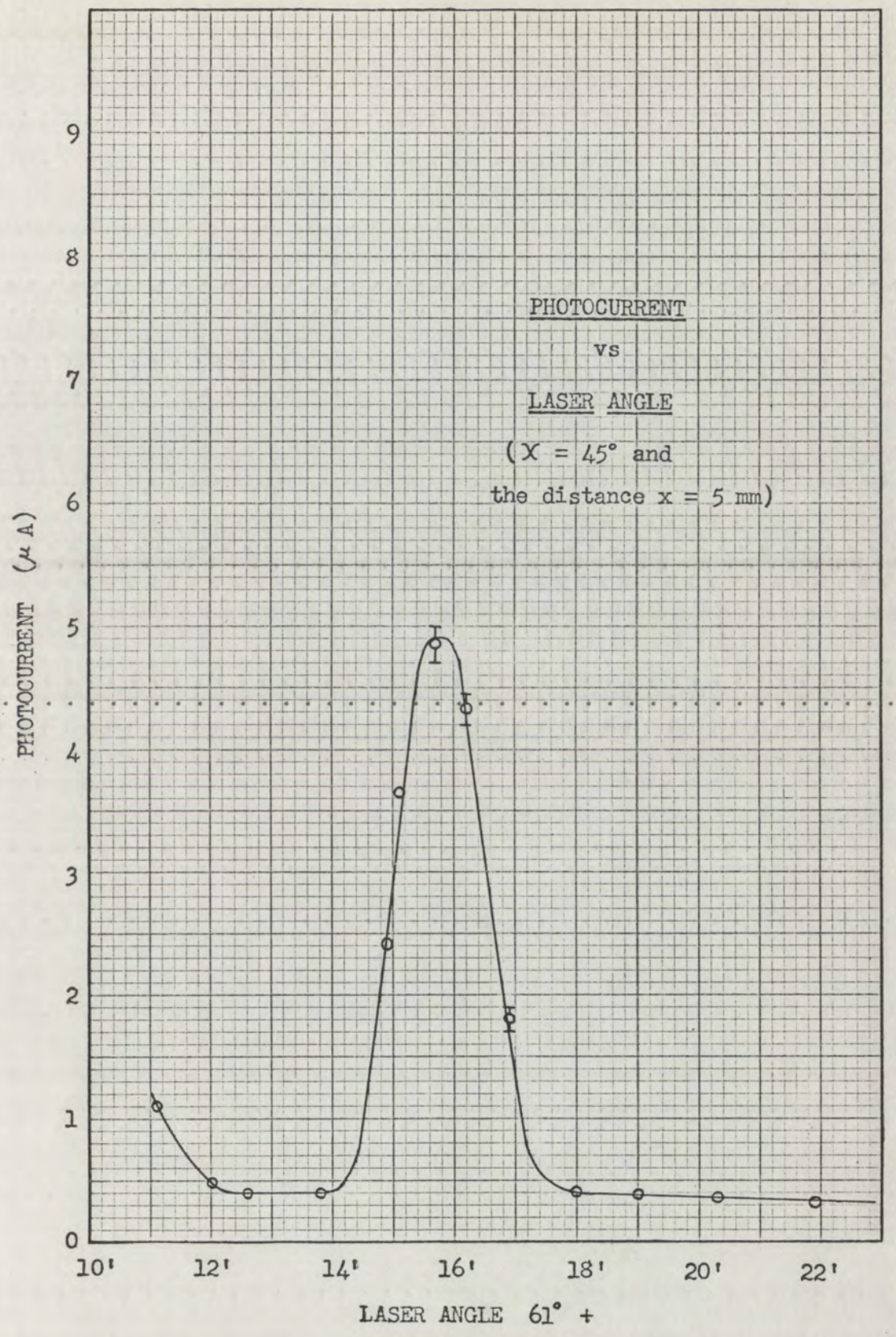


Figure 8. Intensity vs Laser Angle, X = 45°

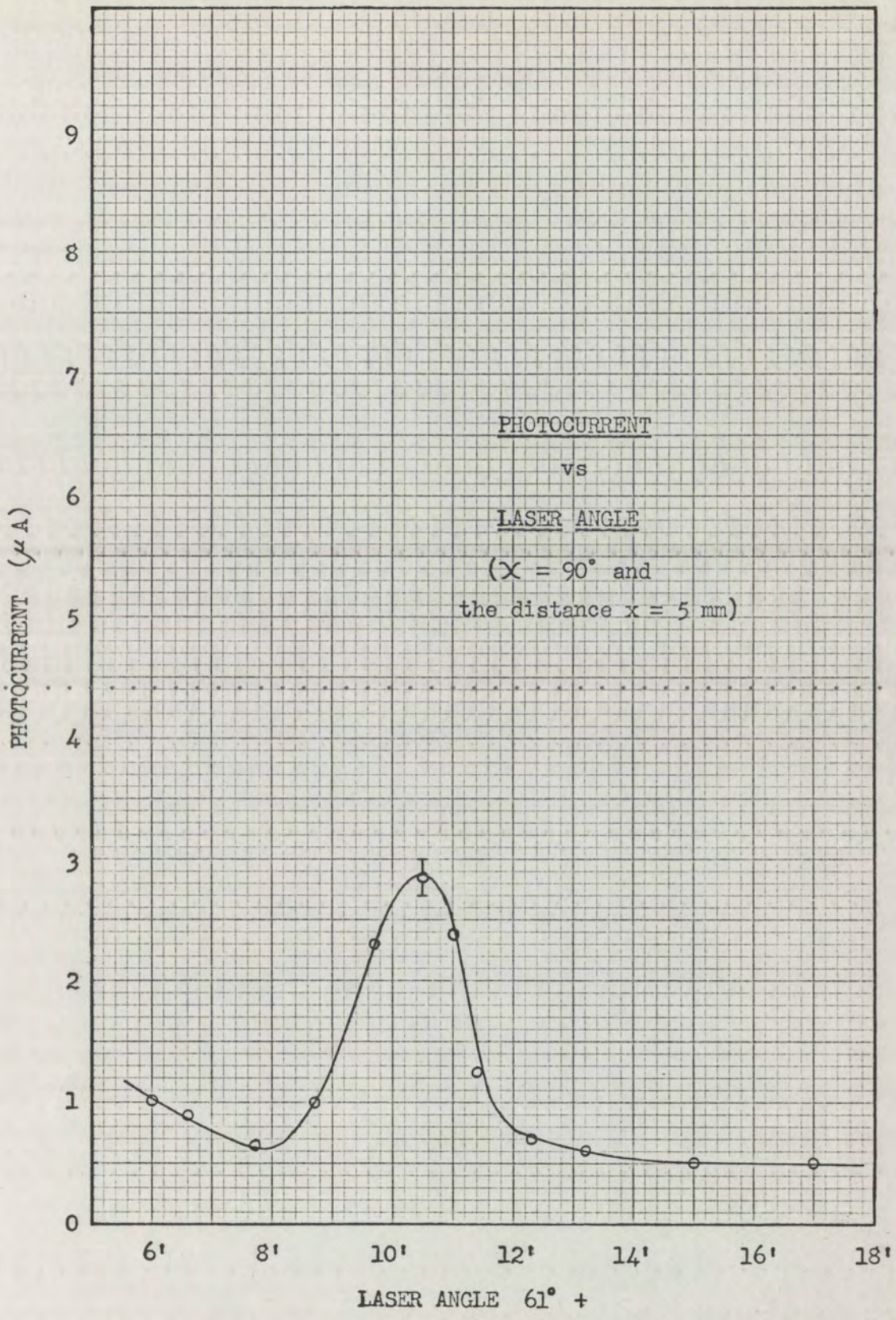


Figure 9. Intensity vs Laser Angle, X = 90°

The intensity of the maximum light at the detector decreases exponentially with distance from the reflected beam (see Figures 10 and 11); whereas the background intensity is roughly constant. The lens and photocell are mounted on a microscope slide using a special adaptor. The slide is positioned to move perpendicular to the reflected beam and in the plane of incidence. The lens holder is aligned parallel to the reflected ray by letting the beam just graze the edge of the lens holder. That position is the closest that the lens and photocell can approach the reflected beam without reflections from the lens holder entering the detector unless the lens is partially masked with an opaque material. The zero distance is taken to be the point where the edge of the reflected beam is at the nearest edge of the open area of the lens; however, the zero point is arbitrary in determining exponential behavior. The slide is then moved away from the reflected ray, and the detector current recorded at various distances. Alternatively, the slide is run out from the beam and data taken as it gradually approaches the reflected beam. Since the lens admits light over a finite interval, say $x_o$, it is desired to ascertain that exponential behavior would be recorded from an exponential source. If one measures

$$I = \int_{x+a}^{x+b} e^{-kx'}\, dx' \,, \tag{20}$$

with $(b-a) = x_o$, then

$$I = -\frac{1}{k}\left[e^{-k(x+b)} - e^{-k(x+a)}\right] ; \tag{21}$$

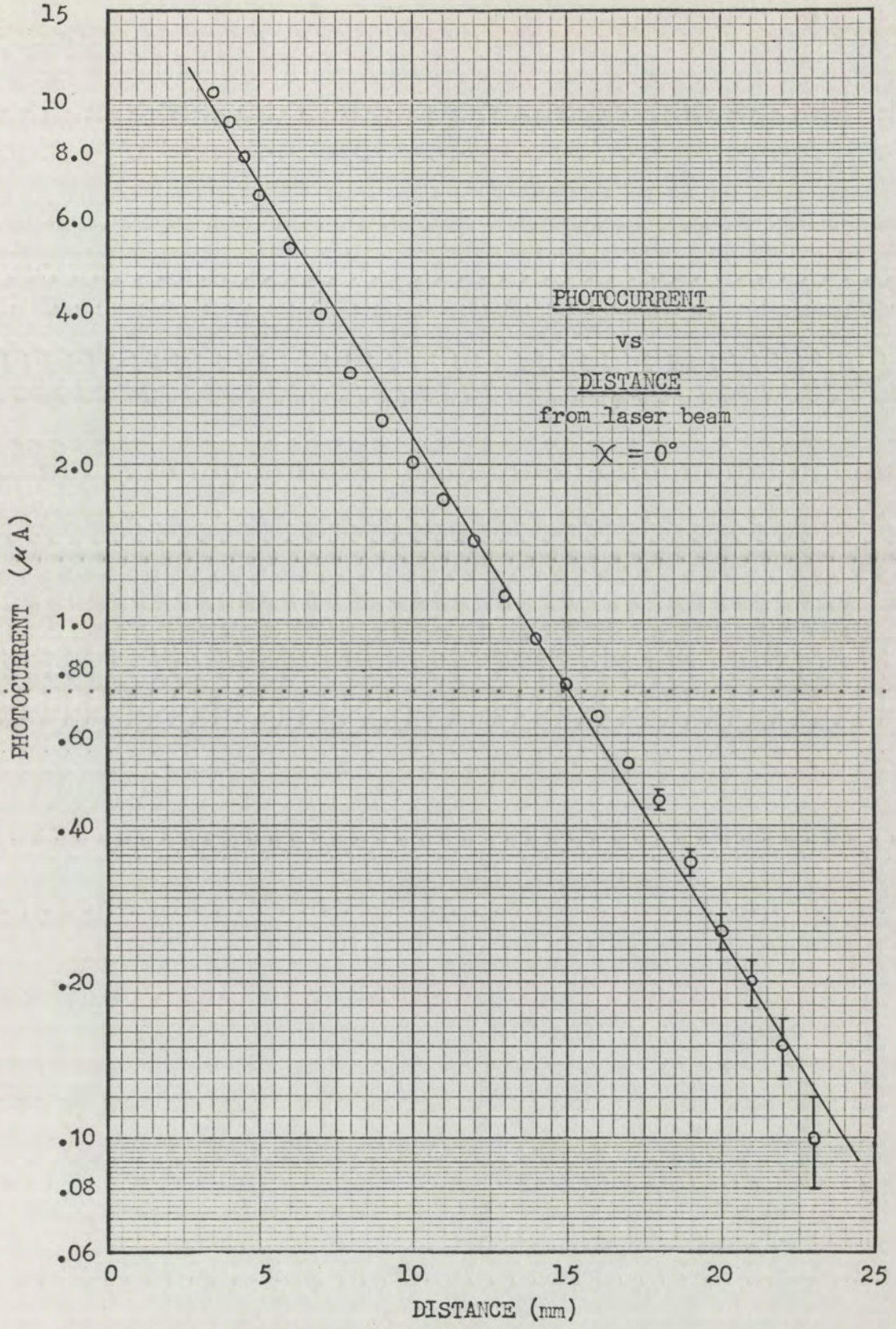


Figure 10. Intensity vs Distance from Laser Beam, X = 0°

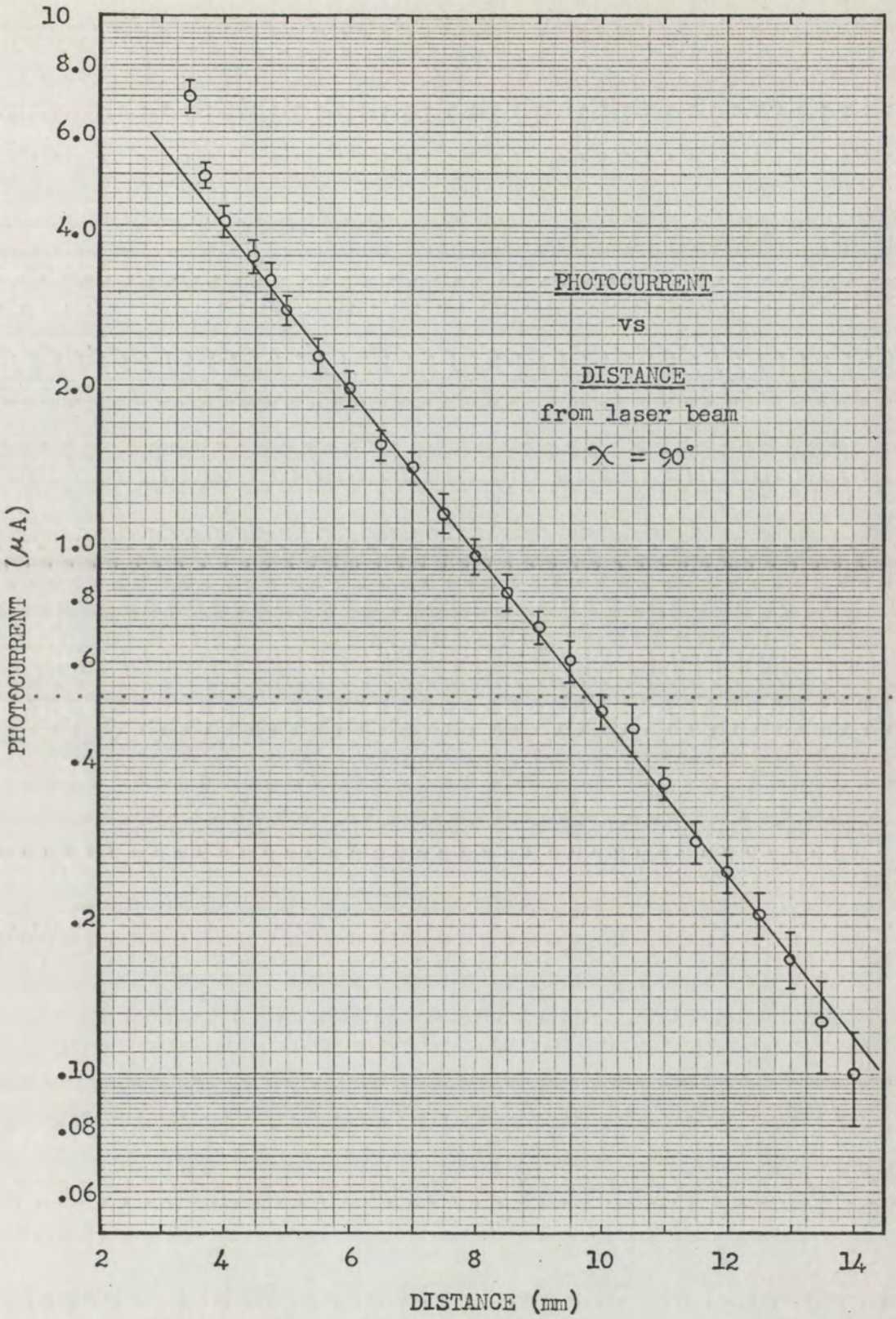


Figure 11. Intensity vs Distance from Laser Beam, X = 90°

$$\therefore\ I = \frac{1}{k} e^{-kx}\left(e^{-ka} - e^{-kb}\right). \qquad (22)$$

Call $$C = \frac{e^{-ka} - e^{-kb}}{k}\ ; \qquad (23)$$

then $$I = C\, e^{-kx} \qquad \text{as desired.} \qquad (24)$$

Exponential behavior does not continue, however, if the upper limit of integration is fixed, as would be the case if the lens were to move far enough from the reflected beam that the black shield in the tank intercepts light rays that would enter the lens. In practice the full lens opening is not employed, but a portion of it varying from 1 to 16 mm. The slopes, -k, of the data shown in Figures 10 and 11 give characteristic lengths, 1/k, in the two cases of polarization:

$$\frac{1}{k_{\parallel}} = 4.44 \pm^{.2}_{.1}\ \text{mm}\ , \qquad (25)$$

and $$\frac{1}{k_{\perp}} = 2.84 \pm .1\ \text{mm}\ . \qquad (26)$$

The values of the slopes obtained from Figures 10 and 11 must be corrected, using information obtained on the performance of the photoconductive cells after a day or more of applied voltage. But since data for these figures are obtained in a single morning, the cell performance is considered to be approximately the same in each case; therefore, the ratio of $1/k_{\perp}$ to $1/k_{\parallel}$ of $0.64 \pm^{.04}_{.05}$ is used. The case $\chi = 0°$ is investigated in much more detail, principally due to the

larger signal that is available. Three separate experiments with the well-seasoned photocell give a weighted average value of $1/k_{\parallel}$ of 3.38 $^{+.3}_{-.2}$ mm. But the characteristic $\gamma$ of the photocell must be taken into account, for if

$$G = L^{\gamma} , \tag{27}$$

$$I = GV , \tag{28}$$

and

$$L = L_o e^{-kx} ; \tag{29}$$

then

$$I = VL_o^{\gamma} e^{-k\gamma x} , \tag{30}$$

so that the value obtained above for $1/k_{\parallel}$ is to be multiplied by the factor $\gamma$. Since $\gamma = 1.20 \pm .04$,

$$\left(\frac{1}{k_{\parallel}}\right)_{best} = 4.05 \, ^{+.5}_{-.4} \text{ mm} . \tag{31}$$

Finally, using the ratio $(1/k_{\perp})$ to $(1/k_{\parallel})$,

$$\left(\frac{1}{k_{\perp}}\right)_{best} = 2.59 \, ^{+.5}_{-.4} \text{ mm} . \tag{32}$$

It is of interest to determine what the characteristic length is at the surface of the water. The geometry is that of Figure 12. Neglecting the tilt of the tank as negligible for this calculation, equation (89) gives $\sin\theta_{\ell} = \cot\theta_c$. Since

$$h = \left(\frac{1}{k}\right) \frac{1}{\cos\theta_{\ell}} , \tag{33}$$

and

$$d = h \cot\theta_c ; \tag{34}$$

then

$$d = \left(\frac{1}{k}\right) \frac{1}{\cos\theta_{\ell}} \sin\theta_{\ell} , \tag{35}$$

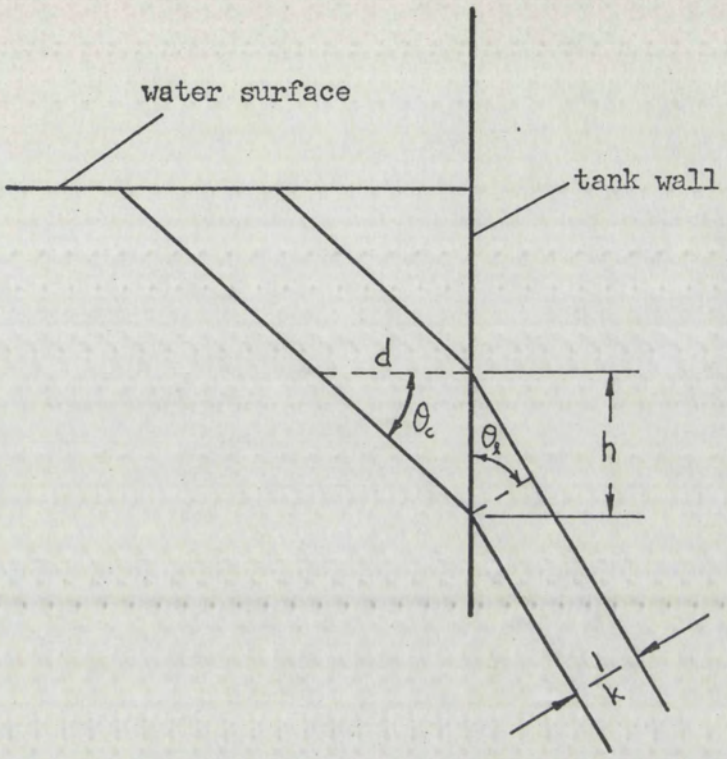


Figure 12. Characteristic Distance

or $$d = \left(\frac{1}{k}\right) \tan \theta_l \quad . \tag{36}$$

Since $\theta_l \doteq 61\frac{1}{3}^\circ$, $\tan \theta_l \doteq 1.83$; (37)

$$\therefore \quad d = \left(\frac{1}{k}\right) 1.83 \, , \tag{38}$$

giving $$d_{\parallel} = 7.4 \, ^{+.9}_{-.7} \text{ mm}, \tag{39}$$

and $$d_{\perp} = 4.7 \, ^{+.9}_{-.7} \text{ mm}. \tag{40}$$

In another experiment the direction of travel of the slide is changed so that the lens and photocell move in a line perpendicular to the plane of incidence, i.e., from one side of the beam to the other. The lens is masked to receive light through a slit which is parallel to the plane of incidence and 2 or $2\frac{1}{2}$ mm wide (slightly less than the width of the reflected beam at that point). With the incident beam linearly polarized with $\chi=45°$, the maximum intensity of the light to the photoconductive cell occurs when the slit is offset from the reflected ray. This result is not found when $\chi = 0°$ or 90°. Figure 13 is a plot of the detector current as a function of position relative to the midpoint of the reflected beam. This point is determined by observing the reflected beam graze equal portions of the extensions of the slit below the edge of the lens holder. The uncertainty in position for equal intensities on either side of the slit is less than 0.02 mm. A similar symmetric result is found for $\chi = 135°$, but with the shift in the opposite direction and somewhat smaller in magnitude. In both cases of polarization, skewed distributions are also obtained giving shifts of the peak to the right and left of the reflected beam. Symmetric and asymmetric distributions are obtained with both slit widths, 2 mm and $2\frac{1}{2}$ mm. The uncertainty in establishing the midpoint in Figure 14 is estimated to be 0.03 mm. The average absolute value of all shifts measured is $0.35 \pm .15$ mm with no preference in magnitude toward either case of polarization.

Evidence Proving Surface Waves

The experimental arrangement does not allow visual observation of the light above the reflected beam; and the low intensity precludes a simple photographic evaluation of its source. It is necessary, there-

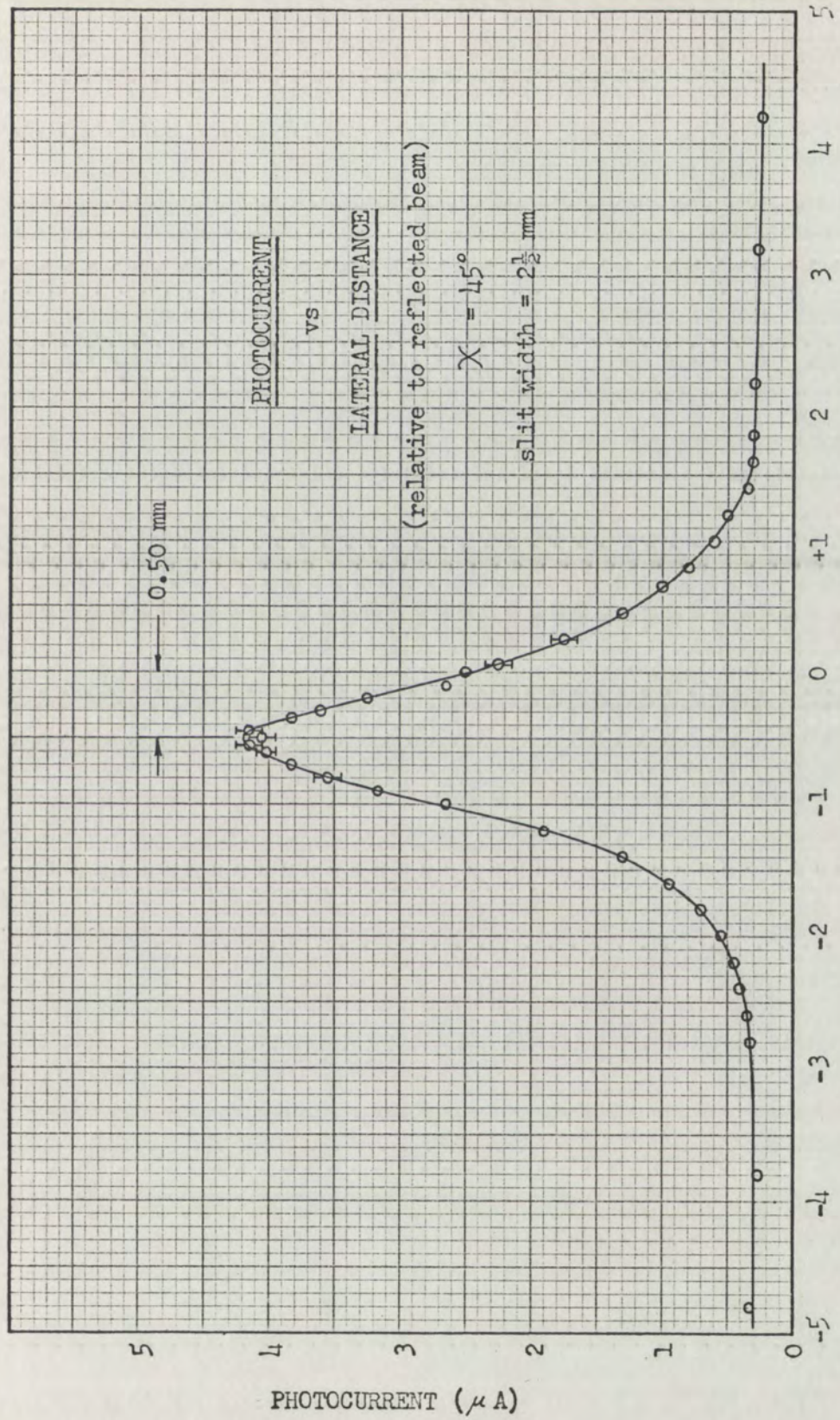


Figure 13. Intensity vs Lateral Distance, Symmetric Distribution

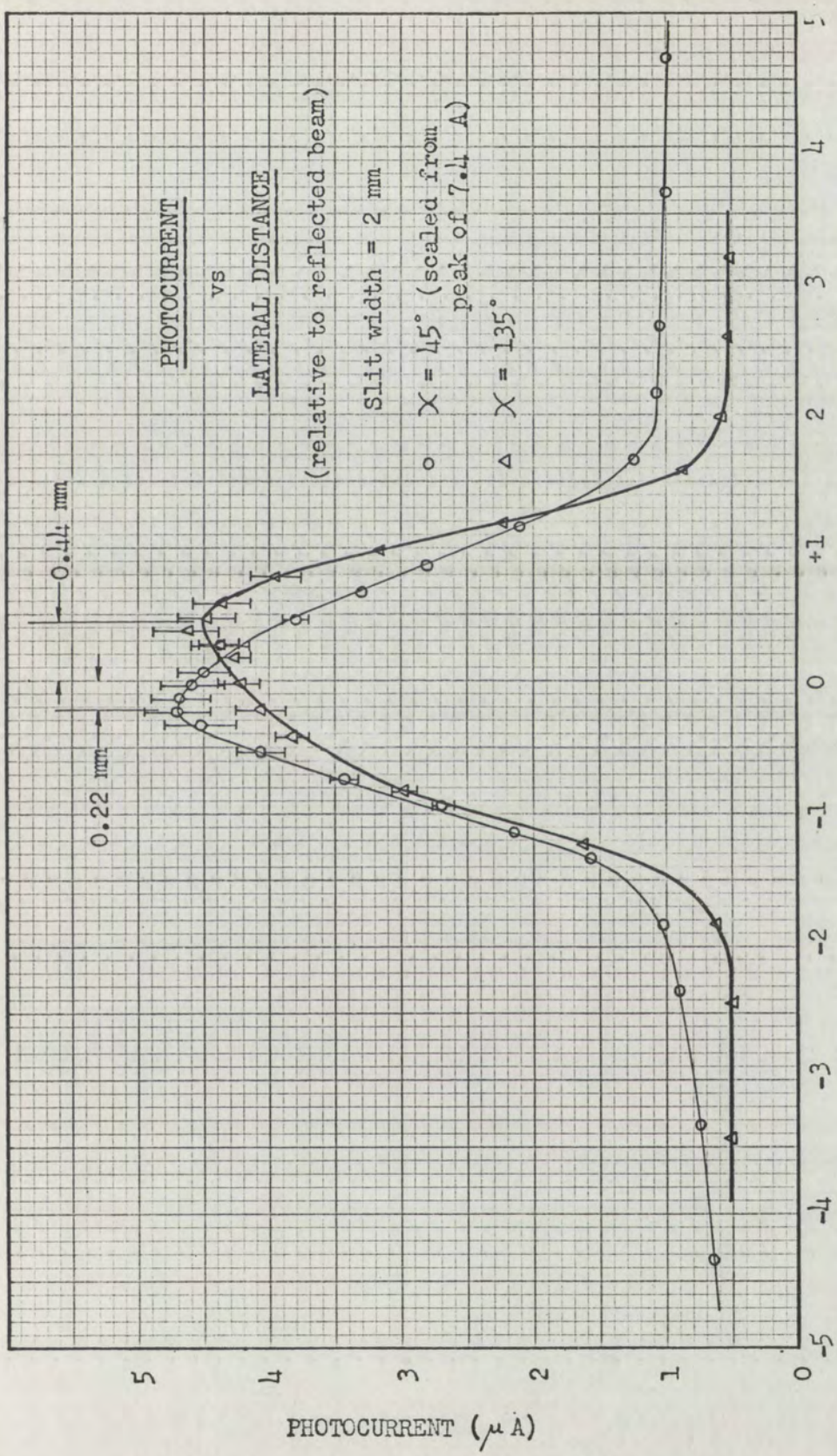


Figure 14. Intensity vs Lateral Distance, Asymmetric Distribution

fore, to establish conclusively by other means the origin of this light. It is asserted that the very characteristics which have been discussed above constitute evidence favoring a surface-wave phenomenon.

The principal source of light approximately parallel to the main beam is light scattered in the water. The path of the beam in water is long enough that some scattered light reaches the photoconductive cell under some conditions, since it enters the detecting apparatus almost parallel to the lens axis. But all the data regarding the detected light contradict a scattered light hypothesis; i.e., that it is observed at a particular angle, the narrowness of the maximum with respect to the laser angle, the polarization effect, and its exponential decay with distance. Light other than that in the peak can be observed at the detector when the reflected ray is near enough the lens or the aperture admitting light to the lens; but this light, interpreted as scattered light, is a slowly varying function of the laser angle and a very rapidly varying function of distance from the reflected beam. This effect is more pronounced when $X = 90^\circ$ than in other cases, a result which would be expected for scattered light; whereas, the opposite result is obtained for the narrow peak.

In addition, many experiments are conducted throughout the observations to eliminate from consideration sources of stray light. One such source is the extraneous light from the laser. The pinhole apparatus is absolutely essential to detect the surface wave signal; without the pinhole everything else is swamped by the extra laser light. With the pinhole in place, one might nonetheless ask if a small amount of off-beam light could be getting through and causing the observed phenomenon; however, the photocell current is rather insensitive to

very small displacements of the pinhole, whether or not the current is at a maximum. If extraneous light from the laser were the source of the signal, even a slight movement of the pinhole would either increase or decrease the intensity at the detector very sharply, depending upon the direction of movement. Also coming from the laser itself is a detectable amount of blue and green light as a diffuse background. The photocell detects a distinct maximum both with and without a Kodak red gelatin filter that is inserted between the aperture and photocell in the lens-photocell combination. These data indicate that extraneous laser light is not the source of the observed narrow maximum. The second source of stray light is reflection and refraction at the meniscus and reflection of the refracted ray from the glass above the water surface. The black strips of paper inserted at the surface, extending 1 to 2 cm below and 2 to 4 cm above the surface, do not reduce the observed peak near the critical angle but do eliminate a much larger and broader peak that is observed without the black paper in cases of partial reflection. Another source of stray light is multiple reflection of the reflected ray inside the water. This source is eliminated by inserting a strip of black paper on the tank floor, anchored by two small pieces of aluminum. Consequently, none of the noticeable sources of stray light are the source of the sharp maximum under consideration. Finally, a front surface mirror is lowered to the surface so that the water is in contact with it. It is aligned parallel to the water surface, a step that can be done very accurately by eye. The lens holder is aligned parallel to the reflected beam as usual, and a search for anything resembling the narrow maximum commences. The background intensity is higher, probably due to diffuse reflection at the mirror,

but not high enough to mask a signal of the same order of magnitude as observed with total internal reflection from the water surface. Several configurations of mirror depth, lens angle, and lens distance from the beam are examined; no result similar to the one described above can be obtained. The maximum is observed again, however, after the mirror is removed and before the plastic cover is replaced.

The experimental evidence for the existence of a surface wave is conclusive. The obvious sources of stray light are shielded without affecting the signal. Light scattered in the water is shown not to be a possibility; indeed, it can be observed independently. The experimental conditions are duplicated with a metal surface mirror reflecting the light, and no comparable signal is obtained. Finally, the probability that some anomalous light source would have all the properties observed is considered to be negligibly small.

## DISCUSSION OF RESULTS

Detection of surface waves at angles of incidence very near the critical angle corroborates results by Osterberg and Smith [6]; however, this experiment went further in determining properties of the surface wave phenomenon. There has been no general theory of surface waves published, nor is the exact mechanism of transfer known. It is suggested that this "long distance" transmission of energy along the surface is related to the small translation of a beam of light measured by Goos and Hänchen [3] and discussed theoretically in several references [2,4,5,8]. Renard [5] obtains an expression for this shift assuming a transfer of energy from one side of the beam to the other. Such a transfer could occur by the same mechanism that produces the effects measured in these experiments; moreover, the results obtained here indicate that if a shift were produced in that manner, it would be very small. There is one piece of evidence in particular that points to a connection between the two effects. The intensity of the surface waves produced when the angle of polarization of the incident light is 45° is observed to be peaked off the center of the reflected beam, measured perpendicular to the plane of incidence. This result correlates with Fedorov's prediction that there can be a perpendicular component of the surface wave accompanying total internal reflection of infinite plane waves [4].

Does one expect an exponential function to describe the distance

distance of travel along the surface? Consider a surface wave launched at some point. One observes the phenomenon by looking at the surface at the critical angle, so it is known that somehow the energy re-enters the water. The simplest theory is that there is a uniform probability per unit distance for the surface wave to enter the denser medium. But this formulation is equivalent to that of passage of radiation through matter, radio-active and biological decay, etc.; i.e., the attenuation is exponential.

There are many questions raised in connection with surface waves. Where are they actually, in the rarer medium, trapped in a surface layer of the denser medium, or in intimate contact with both media? These experiments indicate little difference in their behavior whether the surface is clean or dirty. How do surface waves and those refracted into the denser medium satisfy boundary conditions? Theoretical examination is certainly called for. It would be of considerable interest to perform these experiments with more finely collimated light, light of different wavelengths and polarization properties, and with more precise equipment. It would be desirable, for example, it verify Osterberg and Smith's result for surface wave intensity as a function of the angle of incidence. One hopes that this thesis may stimulate further research in the field of surface wave phenomena.

APPENDIX I

## REFLECTION AND REFRACTION IN VECTOR NOTATION

The material presented in this appendix generally follows the treatment by F. Fedorov [4]. Writing plane waves in the following form:

$$\vec{E} = \vec{E}_0 e^{-i\phi}, \tag{41}$$

$$\vec{H} = \vec{H}_0 e^{-i\phi}, \tag{42}$$

$$\phi = \omega\left(t - \frac{\vec{m}\cdot\vec{r}}{c}\right), \tag{43}$$

where $\vec{E}_0$ and $\vec{H}_0$ are in general complex quantities, Maxwell's equations for plane waves in non-magnetic media ($\mu = 1$) have the form

$$\vec{D} = \varepsilon \vec{E}, \tag{44}$$

$$\vec{D} = -\vec{m} \times \vec{H}, \tag{45}$$

$$\vec{H} = \vec{m} \times \vec{E}, \tag{46}$$

where $\vec{m} = n\,\vec{n}$ is the "refraction vector", n is the index of refraction, and $\vec{n}$ is the unit vector normal to the wave front. The vector $\vec{m}$ is related to the dielectric constant, $\varepsilon$, by the relation

$$\vec{m}^2 = \varepsilon . \tag{47}$$

The Poynting vector $\vec{P}$ is given by

$$\vec{P} = \frac{c}{16\pi}\left(\vec{E} + \vec{E}^*\right) \times \left(\vec{H} + \vec{H}^*\right) . \tag{48}$$

Consider the case of a wave incident on the boundary between two

dielectric media; let the indices 0, 1, and 2 refer to the incident, reflected, and refracted waves respectively. Let $\vec{h}$ be the unit vector normal to the interface. The geometric law of reflection and Snell's of refraction are written in the following form:

$$\vec{m}_0 \times \vec{h} = \vec{m}_1 \times \vec{h}, \tag{49}$$

$$\vec{m}_0 \times \vec{h} = \vec{m}_2 \times \vec{h}; \tag{50}$$

and since the three expressions are equal, Fedorov denotes this quantity by the vector $\vec{a}$; i.e.,

$$\vec{m}_0 \times \vec{h} = \vec{m}_1 \times \vec{h} = \vec{m}_2 \times \vec{h} = \vec{a} . \tag{51}$$

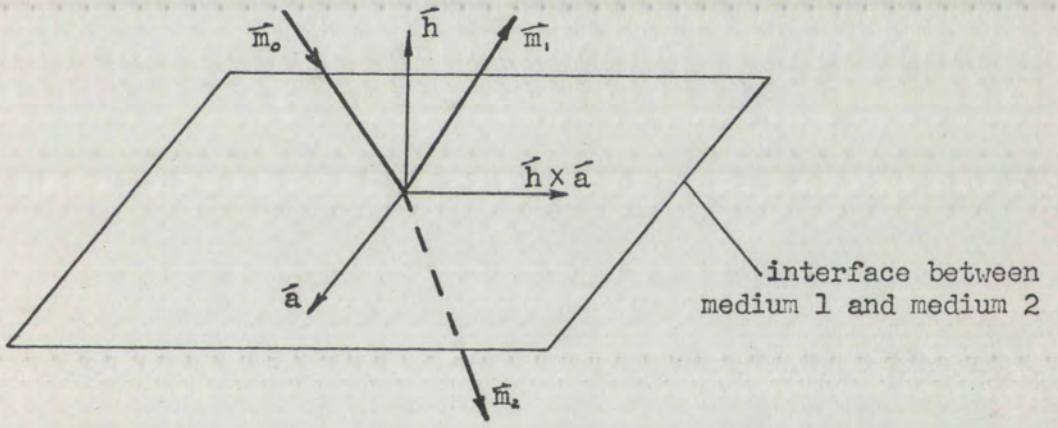


Figure 15. Fedorov's Vectors

Since the three vectors $\vec{m}_0$, $\vec{m}_1$, and $\vec{m}_2$ are co-planar with the plane formed by $\vec{h}$ and $\vec{h} \times \vec{a}$, it is evident that each one can be resolved into components in those directions.

$$\vec{m}_i = (\vec{m}_i \cdot \vec{h})\vec{h} + \frac{[\vec{m}_i \cdot (\vec{h} \times \vec{a})](\vec{h} \times \vec{a})}{(\vec{h} \times \vec{a})^2}, \tag{52}$$

$$\vec{m}_i \cdot (\vec{h} \times \vec{a}) = \vec{a} \cdot (\vec{m}_i \times \vec{h}), \tag{53}$$

$$\vec{a} \cdot (\vec{m}_i \times \vec{h}) = \vec{a} \cdot \vec{a} = \vec{a}^2 ; \tag{54}$$

but $\vec{a}^2 = (\vec{h} \times \vec{a})^2$ since $\vec{h}$ is a unit vector and they are orthogonal;

$$\therefore \quad m_i = (\vec{m}_i \cdot \vec{h})\,\vec{h} + \vec{h} \times \vec{a} \; . \tag{55}$$

Let $\vec{m}_i \cdot \vec{h}$ be denoted by $\eta_i$. Since $n_0 = n_1$, clearly

$$\eta_1 = -\eta_0 \; ; \tag{56}$$

and
$$\eta_2 = \vec{m}_2 \cdot \vec{h} = n_2 \cos\theta_2 \; . \tag{57}$$

$$n_2 \cos\theta_2 = \sqrt{n_2^2 - n_2^2 \sin^2\theta_2} \; , \tag{58}$$

but
$$\vec{a} \cdot \vec{a} = (\vec{m}_2 \times \vec{h})^2 \; ; \tag{59}$$

$$\therefore \quad \vec{a} \cdot \vec{a} = (n_2 \sin\theta_2)^2 \; , \tag{60}$$

using (58) and (60), $\eta_2 = \sqrt{n_2^2 - \vec{a}^2}$ . (61)

Total reflection occurs when $\eta_2$ is imaginary; i.e., when

$$n_2^2 - \vec{a}^2 \leq 0 \; . \tag{62}$$

In that case, $\vec{m}_2$ is written

$$\vec{m}_2 = \vec{h} \times \vec{a} + i\eta\vec{h} \; , \tag{63}$$

where $\eta = +\sqrt{\vec{a}^2 - n_2^2}$ . The electric field of each of the three waves is written in the form

$$\vec{E}_i = A_i\,\vec{a} + B_i\,(\vec{n}_i \times \vec{a}) \; . \qquad i = 0,1,2 \tag{64}$$

$A_i\vec{a}$ is the component perpendicular to the plane of incidence, and $B_i(\vec{n}_i \times \vec{a})$ is the component parallel to the plane of incidence. It can be shown that the Fresnel formulae for the amplitudes $A_i$ and $B_i$ have the form

$$\frac{A_0}{\vec{a} \cdot (\vec{m}_1 \times \vec{m}_2)} = \frac{A_1}{\vec{a} \cdot (\vec{m}_2 \times \vec{m}_0)} = \frac{-A_2}{\vec{a} \cdot (\vec{m}_0 \times \vec{m}_1)} \; ; \tag{65}$$

and $$\frac{B_0/A_0}{\vec{n}_0 \cdot \vec{n}_2} = \frac{B_1/A_1}{\vec{n}_1 \cdot \vec{n}_2} = \frac{B_2/A_2}{\vec{n}_2 \cdot \vec{n}_2} \quad . \tag{66}$$

Finally, the equation for the Poynting vector in an isotropic non-magnetic dielectric is obtained. Using (46) and (48),

$$\vec{P} = \frac{c}{16\pi} \left(\vec{E} + \vec{E}^*\right) \times \left(\vec{m} \times \vec{E} + \vec{m}^* \times \vec{E}^*\right); \tag{67}$$

$$\vec{P} = \frac{c}{16\pi} \left[\vec{E} \times (\vec{m} \times \vec{E}) + \vec{E} \times (\vec{m}^* \times \vec{E}^*) + \vec{E}^* \times (\vec{m} \times \vec{E}) + \vec{E}^* \times (\vec{m}^* \times \vec{E}^*)\right]; \tag{68}$$

$$\vec{P} = \frac{c}{16\pi} \left\{ \left[\vec{m}(\vec{E} \cdot \vec{E}) - \vec{E}(\vec{E} \cdot \vec{m})\right] + \left[m^*(\vec{E} \cdot \vec{E}^*) - \vec{E}^*(\vec{E} \cdot \vec{m}^*)\right] + \left[m(\vec{E}^* \cdot \vec{E}) - \vec{E}(\vec{E}^* \cdot m)\right] + \left[\vec{m}^*(\vec{E}^* \cdot \vec{E}^*) - \vec{E}^*(\vec{E}^* \cdot \vec{m}^*)\right]\right\}; \tag{69}$$

$$\therefore \vec{P} = \frac{c}{16\pi} \left[\vec{m}\vec{E}^2 + \vec{m}^*\vec{E}^{*2} + (\vec{m} + \vec{m}^*)|\vec{E}|^2 - \vec{P}'\right], \tag{70}$$

where $$\vec{P}' = \vec{E}\left[(\vec{E} \cdot \vec{m}) + (\vec{E}^* \cdot \vec{m})\right] + \vec{E}^*\left[(\vec{E} \cdot \vec{m}^*) + (\vec{E}^* \cdot \vec{m}^*)\right]. \tag{71}$$

Since the real parts of $\vec{E} \cdot \vec{m}$ and $\vec{E}^* \cdot \vec{m}^*$ must be zero, $(\vec{E} \cdot \vec{m}) = -(\vec{E}^* \cdot \vec{m}^*)$. Then

$$\vec{P}' = \vec{E}\left[(\vec{E}^* \cdot \vec{m}) - (\vec{E}^* \cdot \vec{m}^*)\right] - \vec{E}^*\left[(\vec{E} \cdot \vec{m}) - (\vec{E} \cdot \vec{m}^*)\right]; \tag{72}$$

$$\vec{P}' = \vec{E}\left[(\vec{m} - \vec{m}^*) \cdot \vec{E}^*\right] - E^*\left[(\vec{m} - \vec{m}^*) \cdot \vec{E}\right]; \tag{73}$$

$$\therefore \quad \vec{P}' = (\vec{m} - \vec{m}^*) \times (\vec{E} \times \vec{E}^*) \; . \tag{74}$$

$$\vec{P} = \frac{c}{16\pi} \left[\vec{m}\vec{E}^2 + \vec{m}^*\vec{E}^{*2} + (\vec{m} + \vec{m}^*)|\vec{E}|^2 - (\vec{m} - \vec{m}^*) \times (\vec{E} \times \vec{E}^*)\right] . \tag{75}$$

APPENDIX II

PHOTOCELL CIRCUIT DETAILS

Photocell Circuit

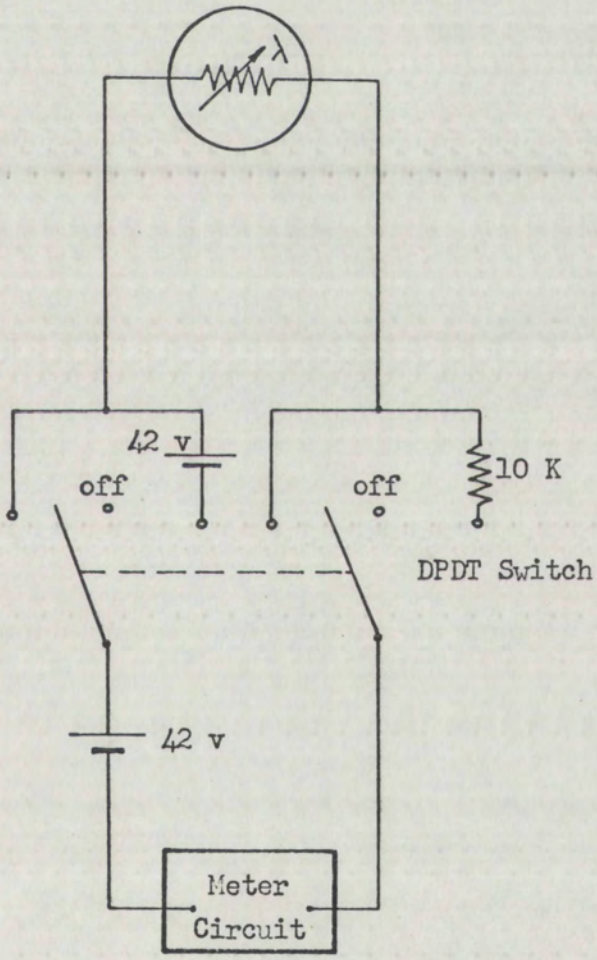


Figure 15. Photocell Circuit

The 10 K ohm resistor is included in series with the photocon-

ductive cell to provide a current limitation; however it introduces excessive nonlinearity when the Clairex -L series cells are plugged into this circuit. Since the Clairex cells also have a higher current rating than does the RCA 4413, the need for a current limiting resistor is not great; consequently, the 10 K ohm resistor is switched out for use with the 42 v circuit used with the Clairex cells.

Meter Circuit

A Weston micro-ammeter having a full scale deflection of 50 $\mu$A is used to measure photocurrents. To provide a wider current capacity, two shunts are designed for use with this meter. Because resistors of the exact values are not available, the shunts are designed for approximate X10 and X100 scale factors; then calibration curves are obtained to get the exact scale factors. The exact scale factors are measured to be 9.69 and 96.6 respectively.

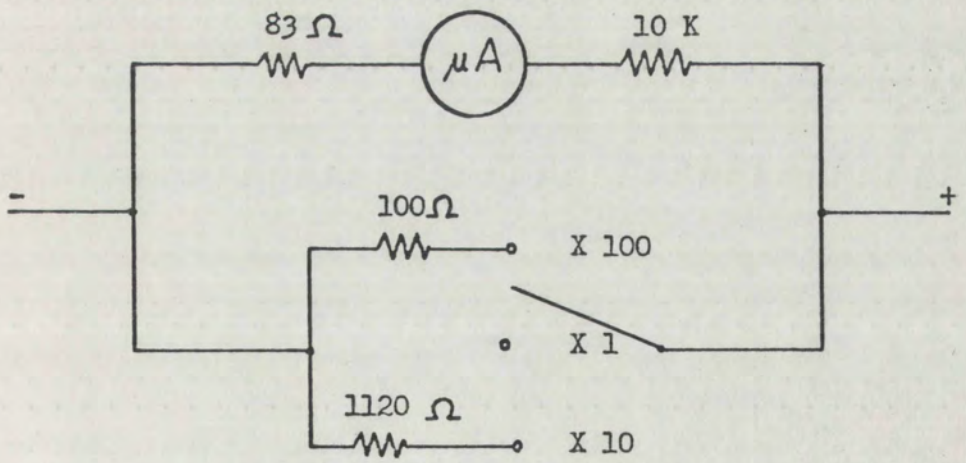


Figure 16. Meter Circuit

## APPENDIX III

## CRITICAL ANGLE

In solid dielectrics it is rather easy to ascertain whether or not a refracted ray exists and to to determine just when it disappears as the angle of incidence approaches the critical angle. The water surface of this experiment introduces a difficulty; namely, the meniscus at the edge of the tank intercepts, reflects, and refracts the refracted beam as it approaches a grazing condition. In addition, a problem common to both solid and liquid dielectrics is that the angular divergence of the light beam introduces a degree of ambiguity in any determination of the critical angle. As a consequence, determination of criticality by observation of the refracted light is quite uncertain, and a more exact method is sought.

### Determination

As pointed out above, evidence of surface waves could give a very accurate determination of the critical angle according to the results of Osterberg and Smith [6]. It is desired to verify Osterberg and Smith's result and to be able to determine the critical angle and small differences from it by an independent method. Since observation of the refracted ray is not suitable for accurate measurements, attention is turned to the reflected ray.

The incident light is linearly polarized due to design of the laser. If the laser is rotated so that the angle between the elec-

tric vector and the plane of incidence is between 0 and $\pi/2$, the reflected light should be either linearly polarized for angles of incidence $\leq \theta_c$ or elliptically polarized for angles of incidence $> \theta_c$. Such an experiment requires that no mirror deflect the laser beam between the laser and the nicol prism which analyzes the reflected ray,[2] because reflection from metals also changes linearly polarized light into elliptically polarized light. Although a beam reflected at less than the critical angle is linearly polarized, the components of the electric vector perpendicular and parallel to the plane of incidence are not equally reflected so that the angle which the elctric vector makes with the plane of incidence, $\chi$, varies as the angle of incidence changes. At the critical angle, however, the reflected ray is linearly polarized at the same angle as the incident ray, since the perpendicular and parallel components of the electric vector are both completely reflected. Thus, if a nicol prism is then aligned with its axis exactly perpendicular to the $\vec{E}$ vector of the reflected wave, light of minimum intensity is transmitted, and any slight change in either direction of the angle of incidence would increase the transmitted light intensity. It is possible to obtain a simple expression for the sensitivity of this determination as the critical angle is approached from above. Equation (19) indicates that a small change in the difference $\epsilon$ between $\theta_i$ $(>\theta_c)$ and $\theta_c$ results in an enhanced change in the phase difference $\delta$ ; i.e., since

---

[2]Alternatively, a mirror could be introduced before the beam enters the tank, providing it is followed by a polarizer to obtain linearly polarized light again.

$$\varepsilon = \frac{1}{8} \tan^3 \theta_c \, \delta^2 , \tag{76}$$

then
$$\Delta\varepsilon = \frac{1}{4} \tan^3 \theta_c \, \delta \, \Delta\delta , \tag{77}$$

or
$$\Delta\delta = \frac{\Delta\varepsilon}{\frac{1}{4} \tan^3 \theta_c \, \delta} ; \tag{78}$$

but since
$$\frac{1}{4} \tan^3 \theta_c \, \delta \ll 1 , \tag{79}$$

$$\Delta\delta = N \Delta\varepsilon , \tag{80}$$

where N is large, thus amplifying the change in the phase difference $\delta$, which is essentially what is measured.

The laser is rotated so that the electric vector of the beam makes an angle of about 45° with the plane of incidence. The laser angle is adjusted so that the angle of incidence is definitely greater than critical—a step which can be done by increasing the laser angle just beyond the point where all evidence of refracted light disappears. Then the nicol prism and mirror are placed in the reflected beam, the function of the mirror simply being to direct the analyzed beam to a convenient point for visual or electronic detection. The preliminary adjustments are most easily accomplished by observing the intensity of the beam as it impinges on a white card. The angle of rotation of the nicol prism with respect to the reflected ray is then adjusted to minimize the observed light intensity. Since the totally reflected

beam is somewhat elliptically polarized, this preliminary minimum is relatively bright. The laser angle is then adjusted to minimize further the intensity of the analyzed beam. This process is repeated until a further decrease in the angle of incidence results in an increase in intensity.. Taking the resulting minimum condition as the criterion for the center of the beam at the critical angle gives somewhat ambiguous results, inasmuch as the brightness of refracted light varies considerably from occasion to occasion of these experiments. The success of this experiment, therefore, is limited; however, the potential usefulness of this technique is considered great enough to warrant further study. For example, this method could also be used to measure small departures from the critical angle.

One difficulty is that of keeping the reflected ray on the photoconductive cell. A slight change in the angle of incidence not only affects the intensity of the analyzed light, but also its direction. This problem is complicated by the existence of two spurious beams arising from reflections in the glass sides of the tank; these auxiliary beams are easy enough for the eye to distinguish from the main beam but must be prevented from reaching the detecting photocell. The solution to this problem is relatively simple. Coating the sides of the tank with an anti-reflective coating would eliminate the auxiliary beams and allow the photodetector to be placed much nearer the main apparatus where a small change in angle would give a smaller lateral change than at the large distances that are used.

It is believed that one of the reasons that inconsistent results are obtained from this method is that the nicol prism angle of rotation may be such that in order to achieve a minimum, a condition of partial

reflection must be obtained. This situation arises because partially reflected light is linearly polarized, but not at the same angle as light reflected at the critical angle. Elimination of this defect involves improved experimental techniques, which would be more easily achievable with an improved mounting device for the nicol prism. There may be other factors pertaining to the limited success of this experiment, but no clue as to their origin has been unearthed.

Measurement

The previous discussion applies to a technique for determining when the critical angle has been attained. Of considerable interest is a measurement of the critical angle itself. The equipment has, in principle, the capability of making this measurement, providing the condition of criticality can be attained precisely by some method. Two problems inherent in the equipment greatly reduce the precision of any such measurements. The laser mounting wheel, if there were no backlash in it, could measure the angle of the laser beam to within a fraction of a minute. Since the critical angle is a function of the index of refraction, a value for the critical angle can be derived from the laser angle measurement alone, providing the tank wall is vertical at the point of beam entrance. Consider the general case, shown in Figure 18, where the tank wall makes a small angle $\alpha$ with the vertical. Let the angle of incidence at the water surface be the critical angle, $\theta_c$. Let the measured laser elevation be $\theta_l$, and denote the angle of refraction in the glass by $\beta$. Let the indices of refraction of glass and water with respect to air be $n_g$ and $n_w$ respectively. Then, by Snell's Law,

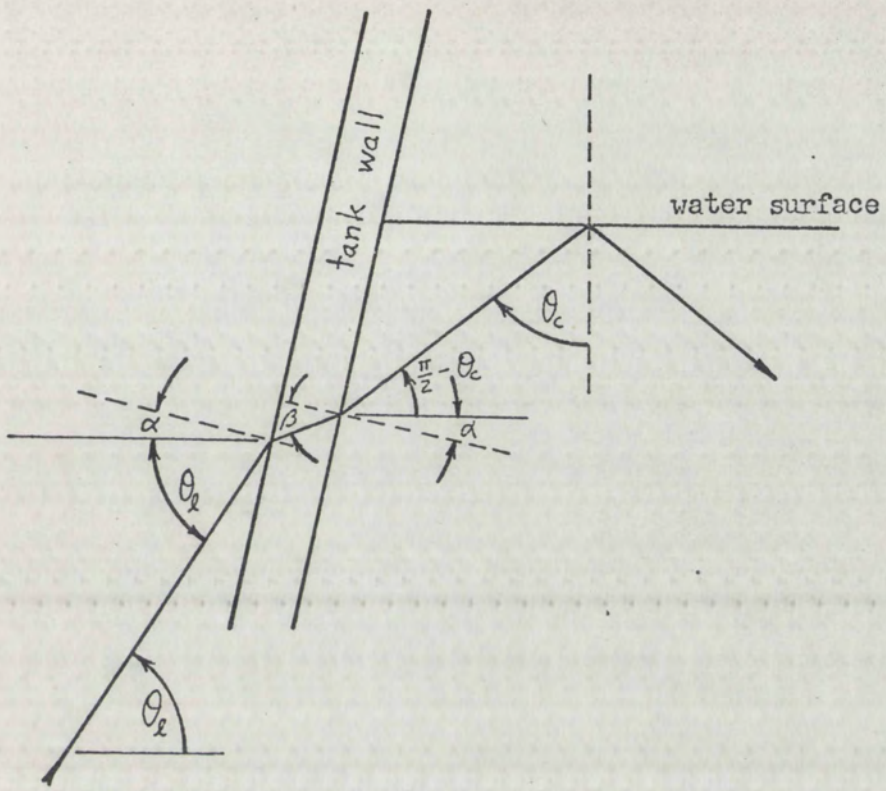


Figure 18. Measurement of the Critical Angle

$$n_g \sin\beta = n_w \sin\left(\alpha + \frac{\pi}{2} - \theta_c\right) , \tag{81}$$

and

$$n_g \sin\beta = \sin\left(\theta_\ell + \alpha\right) . \tag{82}$$

Combining and rewriting,

$$n_w \sin\left[\frac{\pi}{2} - \left(\theta_c - \alpha\right)\right] = \sin\left(\theta_\ell + \alpha\right) , \tag{83}$$

or

$$n_w \cos\left(\theta_c - \alpha\right) = \sin\left(\theta_\ell + \alpha\right) . \tag{84}$$

Expanding,

$$\cos\left(\theta_c - \alpha\right) = \cos\theta_c \cos\alpha + \sin\theta_c \sin\alpha , \tag{85}$$

and $$\sin(\theta_\ell + \alpha) = \sin\theta_\ell \cos\alpha + \sin\alpha \cos\theta_\ell . \quad (86)$$

Since $\alpha$ is small, neglect terms of higher order in $\alpha$ than first:

$$n_w(\cos\theta_c + \alpha \sin\theta_c) = \sin\theta_\ell + \alpha \cos\theta_\ell ; \quad (87)$$

furthermore, since $\sin\theta_c = \frac{1}{n_w}$,

$$\cot\theta_c + \alpha = \sin\theta_\ell + \alpha\cos\theta_\ell , \quad (88)$$

or $$\cot\theta_c = \sin\theta_\ell - \alpha(1-\cos\theta_\ell) . \quad (89)$$

Although $\alpha \ll \sin\theta_\ell$, it is significant if precise results are desired. The uncertainty in $\theta_c$ can be computed as follows:

$$-\csc^2\theta_c \Delta\theta_c = \cos\theta_\ell \Delta\theta_\ell - \Delta\alpha(1-\cos\theta_\ell) + \alpha\sin\theta_\ell\Delta\theta_\ell \quad (90)$$

where the quantities $\Delta\theta_c, \Delta\theta_\ell$ and $\Delta\alpha$ represent the uncertainties in measurement of those quantities. Since $\alpha$ is taken to be zero, the last term vanishes, and

$$\Delta\theta_c = \sin^2\theta_c \left[(1-\cos\theta_\ell)\Delta\alpha - \cos\theta_\ell \Delta\theta_\ell\right] . \quad (91)$$

Since $\cos\theta_\ell$ is about $\frac{1}{2}$, the uncertainty in the vertical of the tank wall is equally important as the uncertainty in the measurement of the laser angle. By providing a mounting apparatus with negligible backlash and by determining the tank wall vertical within less than a minute of arc, an extremely accurate measurement of the critical angle could be obtained.

An approximate value is obtained; however, using the observation

of surface waves as the criterion for criticality. Osterberg and Smith find that surface waves are generated at angles of incidence sharply peaked 1 sec less than the critical angle. One second represents a much sharper angular resolution than is possible with the equipment used in this experiment; therefore, the condition of maximum surface wave light is taken to indicate that the central rays of the laser beam are at the critical angle. The best value for the laser angle when the angle of incidence is critical is 61° 20' ± 10'. Equation (89) gives $\cot \theta_c \doteq \sin \theta_\ell$ ;

$$\therefore \quad \sin \theta_\ell = .8774 \pm .0014 \; ; \tag{92}$$

$$\therefore \quad \theta_c = 48^\circ \; 44' \pm 3' \; ; \tag{93}$$

and since $n_w = \csc \theta_c$, $\quad n_w = 1.3304 \pm .0010$ . (94)

where $\eta_w$ is the index of refraction of distilled water with respect to air. The value obtained is for the wavelength 6328 Å and a water temperature of 22°C.

## APPENDIX IV

### PHOTOGRAPHY

The experiments consisting of photographic examination of the reflected beam are inconclusive at best and are merely summarized here. The arrangement giving the best results is as follows: A high quality camera lens is used alone in the path of the beam to produce a diverging beam beyond the focal point (assuming the laser beam to be approximately parallel light). The Hasselblad 1000 F camera is operated without any lens but simply records the cross section of the diverged beam. Photographs taken at 1/1000th of a second are considered suitable for photo-densitometer analysis.

In the first series, conducted primarily to gain information on exposure times and techniques, cross sections of partially reflected and totally reflected beams are photographed as well as that of a beam simply traversing the tank with no reflection. In addition photographs are taken when all refracted light is just observed to disappear. Although the desired information on techniques is obtained, no physical information is revealed in this series.

The second series is conducted in conjunction with a surface wave detection experiment. In this series all photographs are of the reflected beam and are taken at 1/1000th second. The plane of polarization of the incident light is at 45° to the plane of incidence. Photographs are taken at two distances from the diverging lens; and the

angle of incidence varies through the surface wave maximum, with photographs taken at both sides of and at the peak intensity. The results of this experiment are more encouraging than those of the first series. The motion of the surface and small disturbances in the path of the laser beam are greatly magnified in this experiment and prohibit quantitative analysis of the film. Although there is no firm evidence for an irregularity at the critical angle, there is a suggestion that it would be worthwhile to pursue this approach further, providing conditions are improved.

## REFERENCES


1. M. Born and E. Wolf, Principles of Optics (Pergamon Press, Inc., New York, 1965), pp. 36-51 (Reflection and Refraction of a Plane Wave)

2. J. Picht, Ann. d. Physik, (5), 3, 433 (1929)

3. F. Goos and H. Hänchen, Ann. d. Physik, (6), 1, 333 (1947)

4. F. Fedorov, Dokl. Akad. Nauk SSSR, 105, 465 (1965)

5. R. Renard, J. Opt. Soc. Am., 54, 1190 (1964)

6. H. Osterberg and L. Smith, J. Opt. Soc. Am., 54, 1073 (1964)

7. T. Fahlen and H. Bryant, J. Opt. Soc. Am.,(to be published)

8. B. Rossi, Optics (Addison Wesley Publishing Co., Inc., Reading, Mass., 1957), pp. 366-387

9. H. Schilling, Ann. d. Physik, (7), 16, 122 (1965)